Pergamon

Journal of Structural Geology, Vol. 20, No. 2/3, pp. 175 to 193, 1998

PII: S0191-8141(97)00083-7
0191-8141/98 $19.00+0.00

Breakdown of feldspar, volume gain and lateral mass transfer during mylonitization of granitoid in a low metamorphic grade shear zone

J. F. HIPPERTT*

Departmento de Geologia, Universidade Federal de Ouro Preto 35400-000, Ouro Preto, MG, Brazil

(*Received* 9 *December* 1996; *accepted in revised form* 2 *September* 1997)

Abstract—In a low metamorphic grade shear zone from Quadrilátero Ferrífero (southeastern Brazil), granitoid rocks have been transformed into phyllonites and mylonites via activation of crystal-plastic processes in quartz and fluid-assisted reaction-softening in feldspars. Quartz deformed by basal $<a>$ and prism $<a>$ slip, with concurrent subgrain rotation recrystallization. Breakdown of matrix plagioclase (An_{22-35}) via mica-producing softening reactions required cationic exchanges between Ca, Na and K, forming replacement perthites in the K-feldspar megacrysts, which occupy around 60% of the original rock volume. Subsequent breakdown of the perthitic plagioclase (An_{12-15}) led to disruption of the megacrysts, enabling strain accommodation that localized the mylonite and phyllonite zones. Domainal volume and mass balance calculations based on major and minor elements indicate only small positive changes in mass and volume (around 15%) in the whole system. However, accentuated differences (ranging from mass and volume losses of 25 and 35% at the margins, to gains of 85 and 95% in the centre, respectively) exist between the individual longitudinal subzones occupied by the different tectonite types. This scenario indicates that deformation proceeded as a nearly isochemical process, although with lateral mobility of major elements (principally Si, Al and K) within the shear zone. These results are different from those previously reported for other granitic mylonites, most of them indicating volume losses in compressional tectonic settings. It is suggested that the extensional tectonic framework attributed to the Moeda–Bonfim shear zone (where mass/volume losses are in principle not required) enhanced the access of fluid and consequent transport of components into the shear zone (principally Fe, Si and K), producing the small gains of mass and volume observed.

INTRODUCTION

Low metamorphic grade shear zones are important routes for fluid channelling (hydrothermal or metamorphically derived) in the upper crust. This is because deformation at these conditions normally generates a dynamically stable porosity that enables fluid connectivity through microfractures, grain boundary films and/or grain edges tubules, forming wetted crystal-fluid microstructures (Urai *et al.*, 1986; Watson and Brenan, 1987; Lee *et al.*, 1991). In contrast, fluid connectivity is not so easily attained in high-grade shear zones where pervasive strain-induced recrystallization and grain boundary migration may inhibit porosity development. Thus, it is expected that shearing at low metamorphic grade conditions occurs in the presence of higher fluid/rock ratios [in the range $10–10^4$:1; see O'Hara (1988), Selverstone *et al.* (1991) and Goddard and Evans (1995)], which contrasts with the relatively dry character attributed to deformation under medium/high metamorphic grades (Bell and Cuff, 1989).

Fluid activity has important effects on deforming rocks. Fluid circulation in shear zones alters rates of chemical and mechanical processes, which in turn influence the dominant deformation mechanisms and rock rheology (Janecke and Evans, 1988). For example, a connected fluid circuit may decrease the flow stress by several orders of magnitude (van der Molen and Paterson, 1979; Murrell, 1985). Fluids may also enable dissolution of quartz, feldspar and carbonates, permitting strain accommodation through volume loss (e.g. O'Hara and Blackburn, 1989; Selverstone *et al.*, 1991; Goddard and Evans, 1995) and mass transfer of SiO_2 and other components (principally alkalis) out of the shear zone (Wintsch and Dunning, 1985; Hippertt, 1994a), apart from enabling feldspar breakdown through mica-producing softening reactions (e.g. White and Knipe, 1978; Dixon and Williams, 1983; Simpson, 1985). Overpressure of fluid also enhances fracture propagation, and may promote softening reactions in parallel with brittle deformation. In the ductile field, the presence of fluid enhances dislocation glide and climb (Griggs, 1974), favouring crystal plasticity and dynamic recrystallization (Tullis and Yund, 1989).

Migrating fluids in the upper crust are normally H_2O-rich, as reflected in the mica-enrichment commonly observed in low metamorphic grade tectonites, the extreme case being the formation of phyllonites. In the past twenty years, special attention has been given in the literature to fluid-assisted transfer of elements during deformation (e.g. Beach, 1980; Winchester and Max, 1984; O'Hara, 1988; Dipple *et al.*, 1990; Marquer and Burkhard, 1992; Goddard and Evans, 1995). These studies have shown that at low metamorphic grade conditions, deformation commonly proceeds as an open system with respect to many major, minor and trace elements, contrasting with the mass conservative shearing more common at medium/high metamorphic grades (Jamtveit *et al.*, 1990). Through mass balance and volume

* CNPq Researcher.

balance calculations, these previous contributions have also characterized volume loss as an effective way to accommodate strain in shear zones related to compressional tectonic regimes. However, the role of mass transfer and volume changes in shear zones related to extensional tectonics has been investigated only in a few papers so far (e.g. Reynolds and Lister, 1987; Glazner and Bartley, 1991). To help fill this gap, this paper describes deformation mechanisms and associated chemical changes in a shear zone produced in an extensional tectonic framework. The results are quite different from those previously reported for compressional tectonics, showing that the tectonic framework may exert an important control on the course of chemical and mechanical processes in shear zones.

GEOLOGICAL SETTING

The Quadrilátero Ferrífero is an Archean granite–greenstone terrain (Schorscher, 1978; Marshak *et al.*, 1992) located in the south portion of the São Francisco craton in southeast Brazil (Fig. 1). The greenstone units consist of Archean metavolcanic rocks covered by Proterozoic metasediments surrounding Archean granitic–gneissic–migmatitic complexes. The region experienced a polycyclic tectonic evolution with alternating compressional and extensional tectonic episodes (Marshak and Alkmin, 1989). The last important tectonic event in the region (0.6 Ga) produced most of the regional structures and also accounted for the thrusting front on the eastern border of the Quadrilátero Ferrífero (Chemale *et al.*, 1994). The contacts between these granitic complexes and the supracrustal sequences are marked by low metamorphic grade shear zones with thicknesses varying between 10 and 200 m. This paper deals with mylonites formed in one of these shear zones.

The Moeda–Bonfim shear zone (Hippertt *et al.*, 1992) is a dip-slip shear zone that extends N–S along the contact between the migmatitic Bonfim complex and the Proterozoic Moeda quartzites in the west limb of the inverted Dom Bosco Syncline, west border of the Quadrilátero Ferrífero (Fig. 1). This shear zone dips at moderate to high angles to the east (Moeda quartzites on the top), with all macro and microstructural kinematic indicators consistently indicating a normal dip-slip movement (Hippertt, 1993). The total thickness of the shear zone is roughly 100 m, affecting both the granitic rocks and the quartzites. Mylonites and phyllonites formed in the quartzite side have been investigated previously (Hippertt, 1994a,b). This paper focuses on the tectonites formed by deformation of the granitic rocks.

The metamorphic conditions of deformation are within the upper greenschist facies ($T \sim 400$–$450^{\circ}C$; $P \sim 4$ kb), as reflected by the absence of crystal-plastic deformation in feldspars, recrystallization by subgrain rotation in quartz, and formation of muscovite as a product of retrometamorphic softening-reactions. Strain determinations by the Fry (1979) method using quartz porphyroclasts, indicate a deformation regime close to plane strain simple shear (maximum $\varepsilon_1 = 0.84$, $\psi = 65^{\circ}$). Evidence for solution-transfer of SiO_2 is given by the noticeable development of phyllonites, the presence of fibrous quartz in cracks and strain shadows, the truncation of porphyroclast edges (by dissolution) and the preferential orientation of quartz *c*-axes at low angles to the stretching lineation (Hippertt, 1994a,b).

Although the strain history of the MBSZ is relatively simple, with evidence for only a single tectonic event accounting for strain localization in this shear zone, only recently has the tectonic setting of the MBSZ (and other normal shear zones of the Quadrilátero Ferrífero) been clarified. Because of the geometric complications caused by inversion of the Dom Bosco syncline, this sheared contact was originally attributed to the 0.6-Gy-old, west-verging thrust front that appears principally on the eastern limit of the Quadrilátero Ferrífero. However, this interpretation has been recently refuted by detailed kinematic investigations showing that normal movements (not thrusting) occurred on this shear zone (Hippertt, 1993). The MBSZ in now correlated with the trend of N–S normal structures created by the extensional tectonic event (1-Gy-old) that produced the ascent of the granitic–migmatitic complexes of the Quadrilátero as well as extensive rifting in the southern portion of the São Francisco craton (Marshak and Alkmin, 1989).

The Moeda–Bonfim shear zone

The MBSZ is heterogeneously strained at outcrop scale, with three major domains developed parallel to the shear zone boundaries. The central domain (about 50 m wide) is composed of homogeneous mylonites on both sides of the contact. In contrast, deformation in the marginal domains (principally on the granitoid side) is strongly heterogeneous, and is marked by the development of spaced phyllonite and mylonite zones (from centimetre to metre scale) separated by predominant protomylonites. The phyllonite layers are composed of muscovite, chlorite and quartz with thicknesses in the order of centimetres to decimetres in the granitoid, but sometimes achieving 2 m in the quartzite side. Microstructural and chemical data have been interpreted to reflect an intense fluid activity that enabled quartz dissolution and mica enrichment in these phyllonites (Hippertt, 1994a), but, interestingly, without producing any significant volume loss (Jordt-Evangelista *et al.*, 1993). Spaced mylonite zones occur in both the granitoid and the quartzite, but are much more noticeable in the granitoid side. The quartz mylonites formed in the quartzite side show a deformation partitioning between crystal-plasticity and solution-transfer as reflected by, among other things, a domainal occurrence of quartz *c*-axes oriented at low angles to the stretching lineation (Hippertt, 1994b; Hippertt and Egydio-Silva, 1996). In

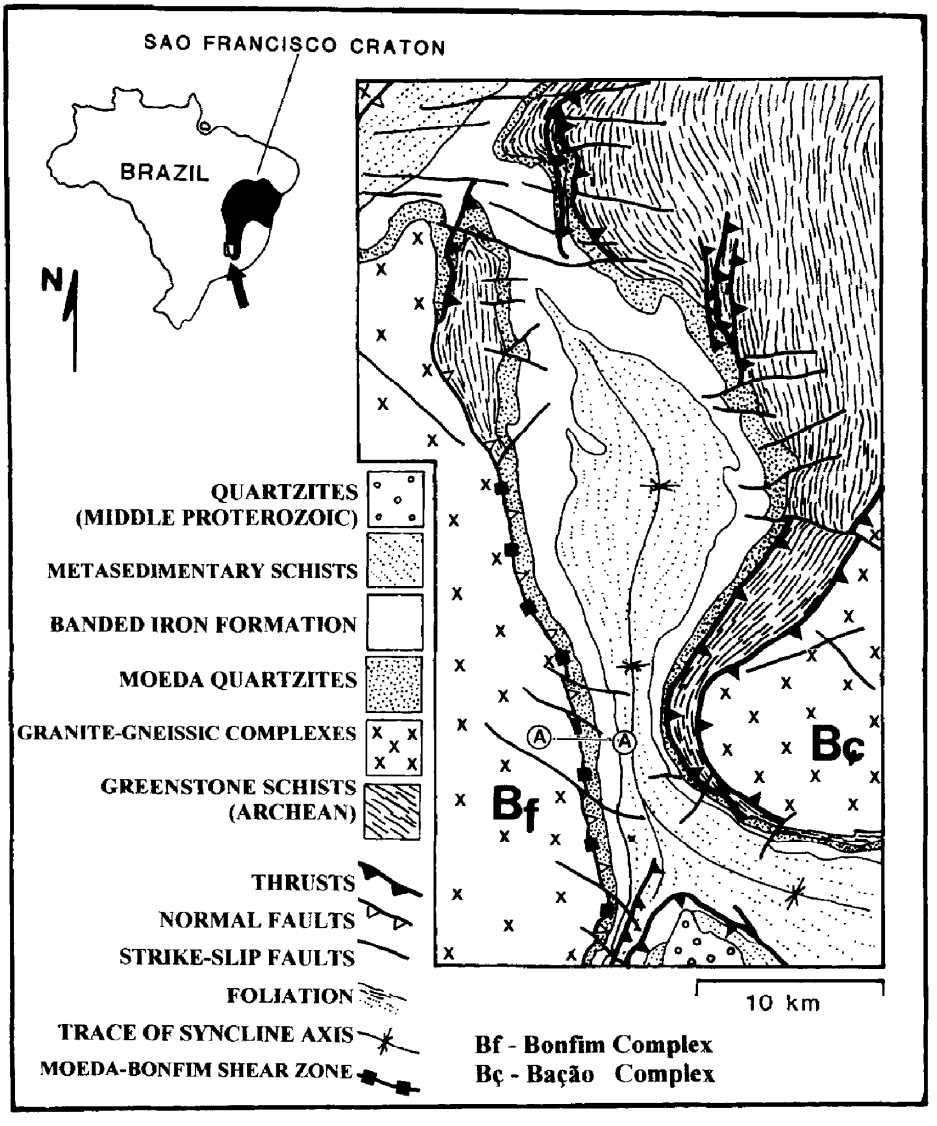

Fig. 1. Geological map of the western Quadrilátero Ferrífero granite–greenstone terrain (southeastern Brazil), showing the location of the Moeda Bonfim shear zone. The line A–A represents the profile across the shear zone where most of research was carried out.

contrast, typical *S–C* mylonites (Berthè *et al.*, 1979) were formed in the granitoid side. They exhibit well-developed sets of *S*- and *C*-foliations making angles between 15 and 45°. A down dip stretching lineation, defined by alignment of muscovite flakes and ribbon quartz, can be observed on both foliations. This paper focuses on one of these mylonite zones (Fig. 2).

This mylonite zone was chosen as it showed a representative range of tectonite types and a well-defined microstructural zoning with increasing strain towards the core. I have collected representative samples of all the internal subzones and investigated the microstructural and chemical variations between these subzones. I assume that most of the processes recognized in this 3-m-wide mylonite zone were also operative in the overall shear zone, although occurring with variable intensities in the different domains of the MBSZ. I also assume that the microstructures of the low strain subzones represent evolving stages that preceded the high-strain microstructures. This is in agreement with the concept that the active segments of shear zones may progressively narrow, if softening processess occur with progressive strain (Means, 1995).

Microstructure

Figure 3 shows the variation in the microstructure across the 3-m-wide mylonite zone investigated. Five different microstructural subzones (here named A, B, C, D and E), which are parallel to the shear zone boundaries, appear from the margins to the centre. They correspond to a progression in strain reflected by grain-size reduction, progressive disappearance of feldspars, decreasing angle between *S*- and *C*- foliations and increasing elongation of polycrystalline quartz ribbons. The distribution of the subzones is asymmetrical, as

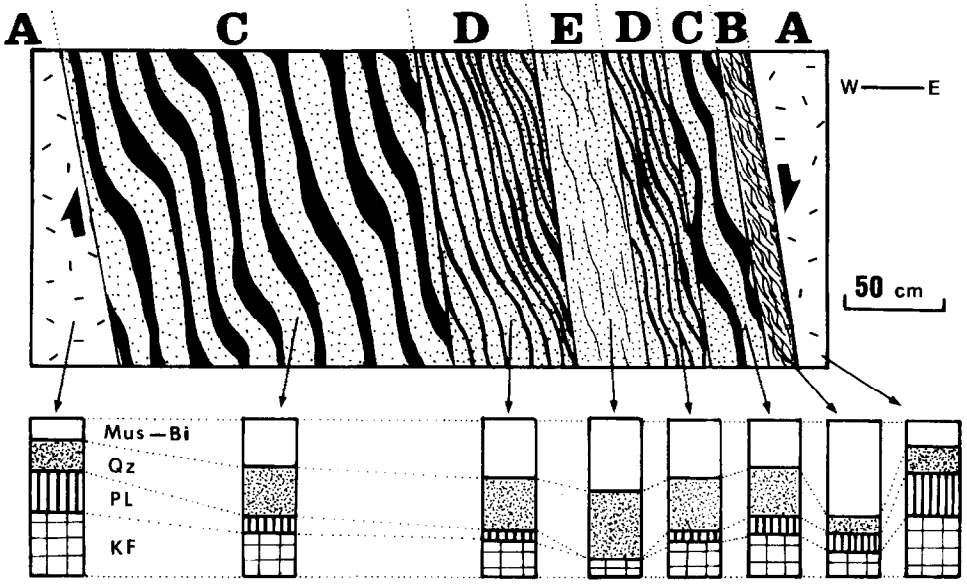

Fig. 2. Schematic profile illustrating the different tectonite types across the 3-m-wide mylonite zone investigated. Letters A–E correspond to the subzones referred to in the text. Compositional variations of micas (Mus–Bi), quartz (Qz), plagioclase (PL) and K-feldspar (KF) are shown in the bottom figure. Note concentration of micas in the shear zone margin and depletion of feldspars towards the centre.

subzone B does not occur on the west margin, and the thicknesses of subzones C and D are very different in each margin. The boundaries of the subzones are generally abrupt.

Subzone A (Fig. 3a) represents the weakly foliated granitoid immediately adjacent to the margins of the mylonite zone. This rock corresponds to the protomylonite that separates the spaced, metre-scale mylonite and phyllonite zones. It is characterized by fracturing (but usually without significant displacement) of K-feldspar megacrysts (perthitic microcline). The matrix plagioclase is partially transformed into an aggregate of epidote, muscovite and quartz. The large quartz aggregates of the original granitoid are deformed internally and show well-developed core-and-mantle microstructures. Biotite is bent and partially transformed into muscovite and chlorite.

Subzone B corresponds to the eastern marginal domain of the mylonite zone. It is characterized by an enrichment in phyllosilicates (principally muscovite, with minor amounts of biotite and chlorite) and depletion in quartz. Small amounts of recrystallized quartz ($<15\%$) occur between the mica-rich folia. There is a strong foliation developed parallel to the shear zone boundaries. This zone is about 15 cm wide with a very sharp contact with the protomylonite, probably reflecting a precursor fracture that localized this boundary of the mylonite zone (cf. Goodwin and Wenk, 1995).

Subzone C shows a coarse layered microstructure where three compositionally distinct layers (feldspar + mica, quartz + mica, pure quartz) occur (Fig. 3b). The layers are approximately 5 mm thick on average. Quartz is finer-grained here than in subzone B and occurs as rectangular grains where associated with mica. The pure quartz layers consist of polygonal, recrystallized grains (average 70 μm) with a small percentage ($<5\%$) of plastically deformed porphyroclasts. The feldspar-mica layers were formed by breakdown of the microcline megacrysts through fracturing and mica-producing softening reactions. The layers of pure quartz were formed by stretching of original quartzose nodules. Formation of the quartz-mica layers is attributed (at least partially) to solution-transfer processes (reprecipitation), as indicated by the quartz c-axis preferred orientation at low angles to the stretching lineation (Tullis, 1989). This structure, comprising well-defined layers of different composition, and therefore with different rheologic behaviours, indicates a scenario of 'laminar' flow with strong deformation partitioning between crystal plasticity (pure quartz layers), reaction-assisted mechanisms (feldspar + mica layers) and solution-transfer creep (quartz–mica layers) during the intermediate stages of progressive strain. Subzone C is 15 cm wide in the east side of the mylonite zone and approximately 1.5 m wide in the west side.

Subzone D shows the same layered structure with layers of the same composition as subzone C. However, the layers are thinner (2 mm thick) and with a smaller grain size relative to subzone C. Another difference is the feldspar content, which is lower than in subzone C, reflecting a more advanced stage of reaction softening. Subzone D is 30 cm wide on the east side of the mylonite zone and 60 cm wide on the west side.

Subzone E corresponds to the highest strain domain of the mylonite zone. It shows a pronounced mica and quartz enrichment associated with feldspar depletion (which contrasts with subzone B, where quartz is depleted). Only a few rounded fragments of microcline occur in the micaceous layers. Plagioclase is absent. The

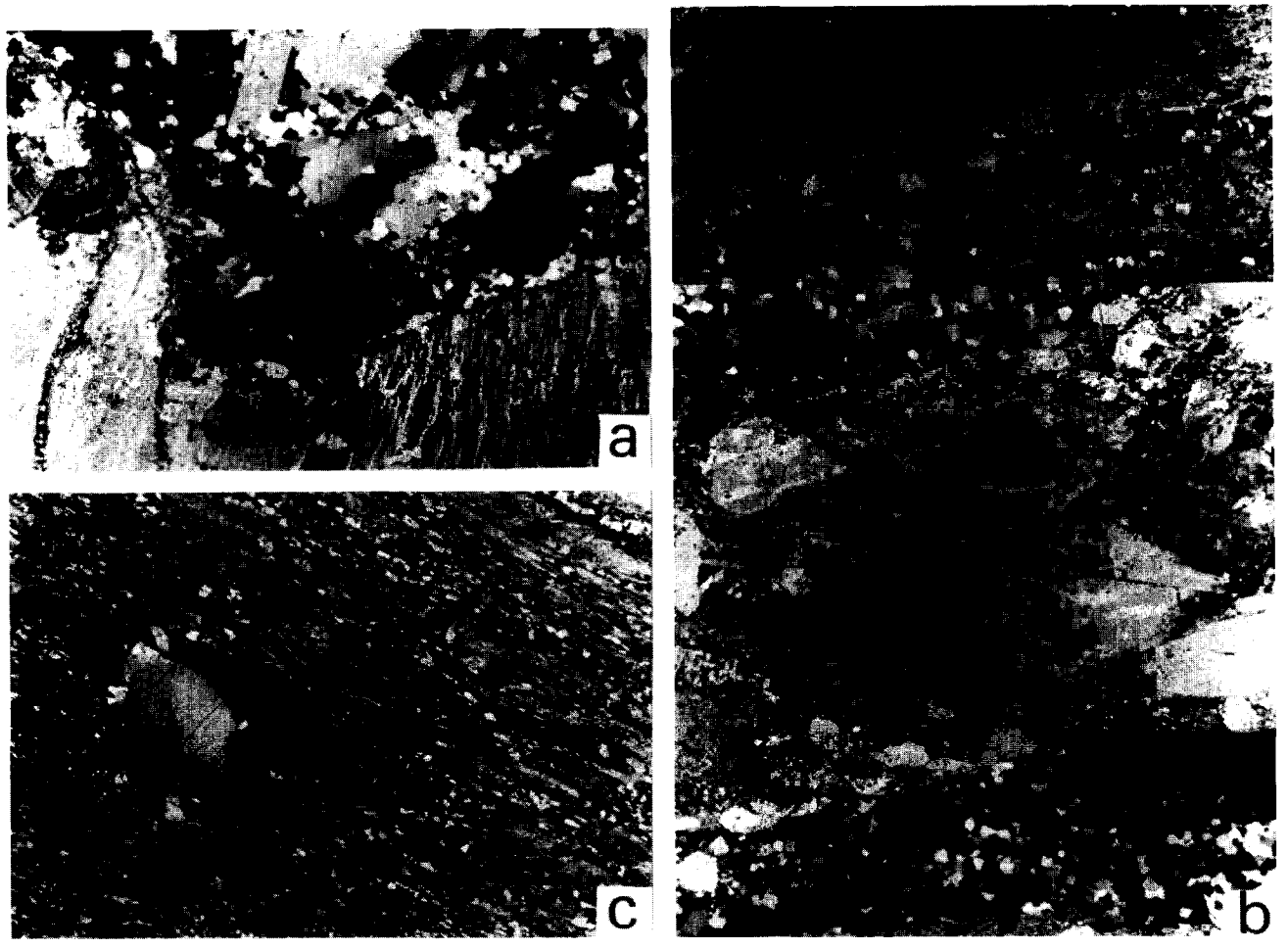

Fig. 3. Microstructure across the mylonite zone. (a) Low-strain domain (Protomylonite, subzone A). Deformed, partially recrystallized quartzose nodules and portions of two fractured K-feldspar megacrysts (bottom) appear on the photograph. Perthitic veinlets in the K-feldspar are oriented parallel to the incipient foliation (vertical in this photo). Base of photo is 2 mm. (b) Intermediate strain (subzone C). This mylonite shows a well-defined tectonic banding at a microscale. Pure quartz bands and feldspar-mica bands appear on the photograph. The latter resulted from fracturing and softening reactions in the original K-feldspar megacrysts. Note that the perthite veinlets in the feldspar fragments are preferentially oriented parallel to the tectonic banding. Base of photo is 1.1 mm. (c) Highest strain (mylonite, subzone E). This mylonite shows an alternating sequence of fine quartz-rich and muscovite-rich bands. Some relic quartz porphyroclasts appear in the quartzose bands. Feldspar is nearly absent. Base of photo is 1.5 mm.

microstructure (Fig. 3c) is much more homogeneous than in the other subzones. The polygonal quartz has a grain size between 30 and 50 μm. Discrete layers of pure mica or pure quartz are locally developed. Subzone E is about 40 cm wide and occurs approximately in the centre of the mylonite zone.

DEFORMATION MECHANISMS

Quartz deformation

Quartz occurs in the undeformed granitoid as coarse (up to 2 cm), polycrystalline aggregates composed of a few individual crystals. In the protomylonite, these aggregates retain their original equidimensional external geometry, but are intensely deformed/recovered internally by crystal-plastic processes. Subgrains are progressively developed from margins to the core, forming typical core-and-mantle microstructures. Deformed, undulating relics occur in the centre of the grains. Dynamic recrystallization of quartz occurred principally by subgrain rotation, as indicated by the similar grain size of subgrain and new grains (White, 1979). Locally, evidence for grain boundary migration recrystallization (e.g. bulged grain boundaries) was also found. With progressive strain, the quartz aggregates were progressively stretched to form layers of polygonal quartz, with a decreasing number of remaining porphyroclasts. The grain size of the recrystallized grains was also systematically reduced from 80 to 30 μm.

Figure 4 shows the preferential orientation of quartz *c*-axis from the protomylonite towards the central subzone E. The recrystallized grains show a strengthening maximum around the Y axis of finite strain, indicating operation of prism $<a>$ slip (Schmid and Casey,

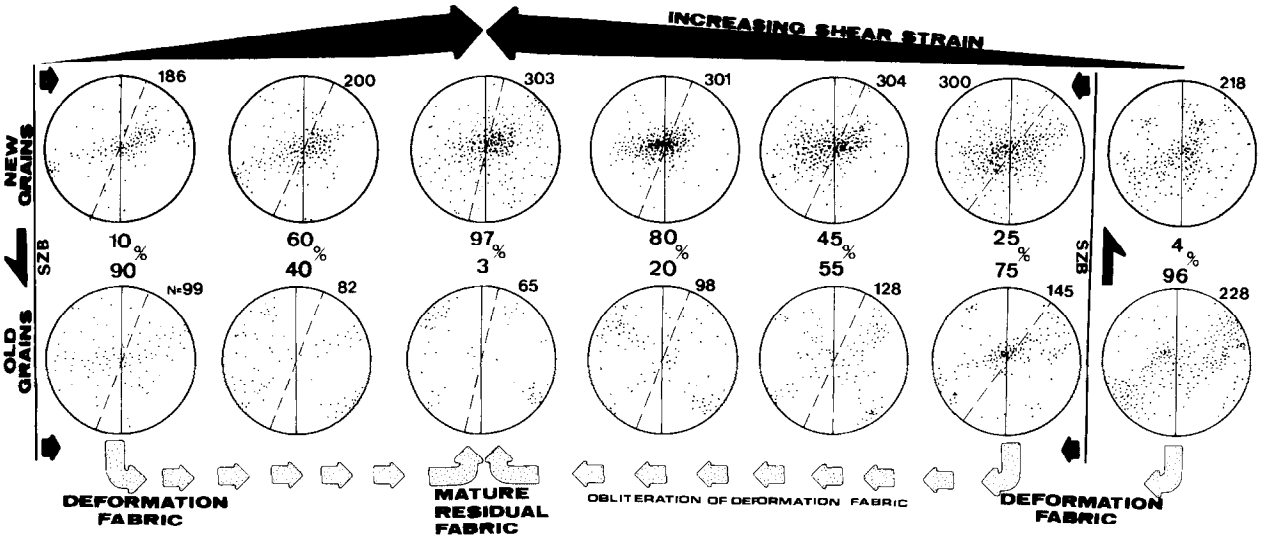

Fig. 4. Evolution of quartz *c*-axis fabrics across the mylonite zone investigated. Percentages indicate the volumetric proportion of porphyroclasts and recrystallized grains. *C*-foliation (solid lines) and *S*-foliation (dashed lines) and shear zone boundaries (SZB) are indicated.

1986). However, prismatic glide in quartz is generally thought to be operative at higher temperatures [amphibolite facies, e.g. Fueten *et al.* (1991)]. Its activation at greenschist facies conditions probably reflects the influx of a syndeformational aqueous fluid in the MBSZ, as the critical resolved shear stress for prism $<a>$ slip is reduced in the presence of water [Blacic, 1975; see also Paterson (1989)]. With progressive strain, there is an increasing contrast between the *c*-axis fabrics of porphyroclasts and recrystallized grains. The porphyroclasts show a weakening *Y* maximum in parallel with the strengthening maxima at 45° with the shear plane. In fact, these maxima represent the most difficult orientations for activation of crystal slip in the $<a>$ directions, as the *a*-axes are in planes where the resolved shear stress is zero (see also Krohe, 1990). Therefore, the *c*-axis fabric present in subzone E (highest strain) is interpreted as representing the last porphyroclasts left behind by selective recrystallization (Hippertt and Borba, 1992).

Feldspar breakdown

The mode of deformation of feldspar in shear zones typically reflects the metamorphic conditions of deformation, where strain-induced crystal-plastic processes predominate at temperatures higher than 500°C, while brittle and reaction-assisted deformation operate at lower temperatures (Fitz Gerald and Stünitz, 1993; Stünitz and Fitz Gerald, 1993). In the investigated shear zone, plagioclase and K-feldspar are destroyed almost exclusively by microfracturing and reaction-assisted mechanisms, although in different ways. Crystal-plastic processes are restricted to occasional bending of twin lamellae of plagioclase. The first grains to show signs of alteration are the matrix plagioclase grains ($An_{22\text{-}35}$), which are progressively transformed into aggregates of epidote, muscovite and quartz. This alteration is present even outside the shear zone, increasing considerably towards the centre of the shear zone. Alteration of the matrix plagioclase seems to occur simultaneously with appearance of albite–oligoclase veinlets ($An_{5\text{-}12}$) in the K-feldspar megacrysts, forming flame and vein perthites. This inference is based on the fact that K-feldspar is not perthitic in granitoid samples where the matrix plagioclase is unaltered. This relationship indicates that the chemical transformation of the matrix plagioclase was associated with the development of perthites. The most likely control on the formation of perthitic plagioclase veinlets is the demand for K that is necessary to form muscovite during plagioclase breakdown. The principal sources of K are the microcline megacrysts, as the biotite content of this rock is very low. Thus, the process can be understood as a combination of reactions 1 and 2 (Orville, 1962; Bryant, 1966; O'Hara, 1988) involving cationic exchange between alkalis, where Na released from the matrix plagioclase is exchanged with K to form albite veinlets in the K-feldspar, while K from the microcline is used to form muscovite in the matrix.

$$\begin{aligned}\text{Oligoclase} + 1.5\ \text{K-feldspar} + 0.5\ H_2O + 4\ H^+ \\ = 2\ \text{muscovite} + 0.5\ \text{epidote} \\ + 11\ \text{quartz} + 4\ Na^+\end{aligned} \quad (1)$$

$$\begin{aligned}\text{K-feldspar} + Na^+ &= \text{albite} + K^+ \\ (109\ \text{cm}^3\ \text{mol}^{-1}) &\quad (101\ \text{cm}^3\ \text{mol}^{-1})\end{aligned}. \quad (2)$$

The process is not isochemical on a thin-section scale, as indicated by the differences in composition between the matrix plagioclase and perthitic plagioclase veinlets. Also, the volume of perthitic plagioclase produced does not correspond to the amount of matrix plagioclase destroyed. Calcium released from plagioclase is initially

retained in epidote (a mineral restricted to the low strain subzones) but has moved out of the mylonite zone at more advanced stages of deformation, where epidote disappears.

The transition to spaced mylonite zones corresponds to the beginning of alteration of the perthitic plagioclase veinlets (again forming muscovite, epidote and quartz), favouring microfracturing and disrupting the host microcline megacrysts (Figs 5 & 6). The disruption of the megacrysts leads to a dramatic increase in strain accommodation, as the microcline megacrysts represent some 60% of the total volume of the rock. Therefore, disruption of the megacrysts should represent the ultimate cause of strain localization in this mylonite zone. In this process, Na and Ca are continuously exchanged with K to form new perthite veinlets (increasingly more sodic) in the K-feldspar fragments. The perthitic veinlets become increasingly finely spaced with progressive strain. However, because the process is not mass-conservative, an increasing mass transfer of Na and Ca out of the mylonite zone occurs (see below). Indeed, the last K-feldspar remnants in the highest strain subzone (subzone E) are totally non-perthitic.

Figure 7 shows the orientation of the perthitic veinlets relative to the kinematic framework of the MBSZ. Most of the veinlets are oriented at low angles to the *S*-foliation, with a secondary maximum at a low angle to the *C*-planes. Overall, the veinlet orientations are spread across an interval of approximately 45° between the *C* and *S* folia, and there is an intensification of the parallelism with the *C* planes towards the centre of the mylonite zone. There is no apparent crystallographic

Fig. 5. (a) Microstructure of subzone D mylonite showing disrupted K-feldspar megacrysts with profusion of perthitic plagioclase veinlets parallel to the shear zone boundary (horizontal in this photo). Base of photo is 1.3 mm. (b) Detail of a perthitic K-feldspar showing intense sericitization (and some displacement) along the perthitic veinlets. The displaced fragments on the left upper corner show a different optical orientation from the host because their movements (arrows) had a rotational component. Base of photo is 210 μm.

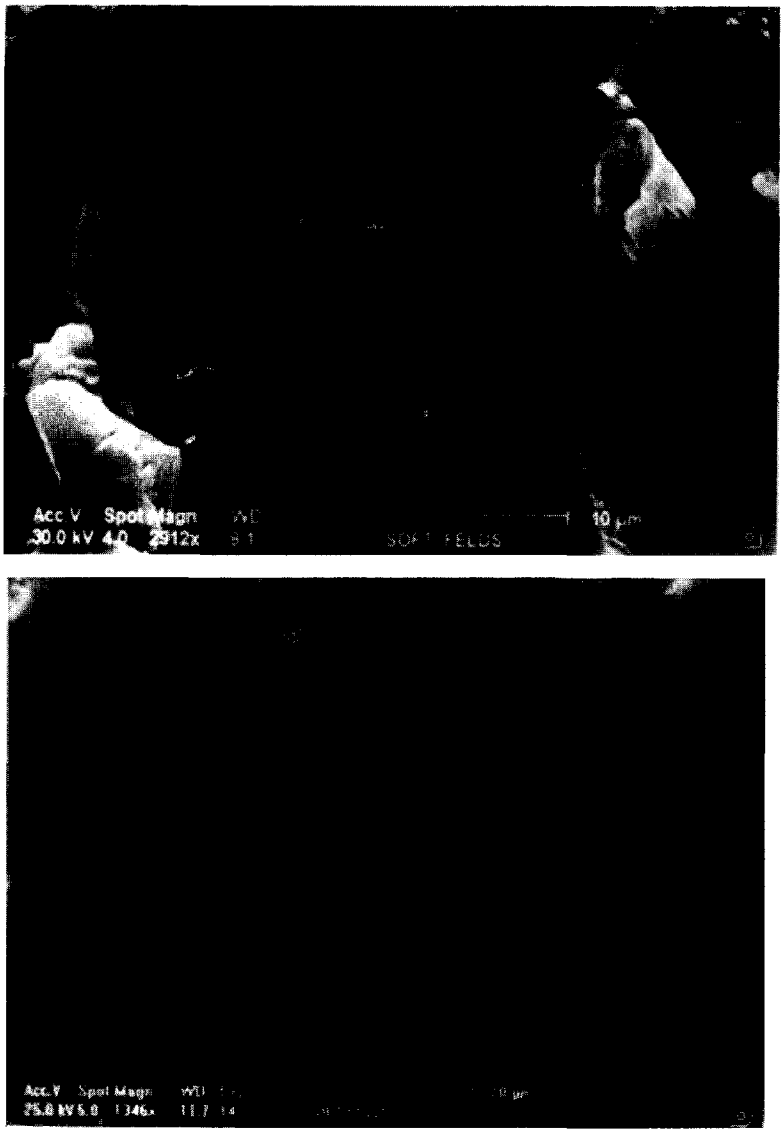

Fig. 6. SEM microstructures (secondary electron mode). (a) A 3-D view of a K-feldspar crystal (K) with thin perthitic veinlets in contact with recrystallized quartz grains (Q) from subzone C mylonite. (b) Detail of a large perthitic veinlet in a K-feldspar megacryst from the protomylonite. Note the crystal of epidote (ep) nucleated in the perthitic veinlet.

control on the orientation of these vein perthites. Interestingly, this contrasts with the orientations recently found in the flame perthites investigated by Pryer and Robin (1995, 1996), which are crystallographic (subparallel to the Murchison plane) and perpendicular to the *S*-foliations (discussed below).

With progressive strain, the average distance between the veinlets decreases as they become thinner and occupy a smaller proportion of the fragment area (Fig. 8). This confirms that the development of the perthitic veins diminishes with progressive strain, in parallel with the progressive migration of Na and Ca out of the shear zone (also corroborated by mass balance calculations). The global process should therefore be envisaged as a progressive alteration of the perthitic veinlets disrupting the K-feldspar, with simultaneous formation of a new generation of thinner and more sodic veinlets in the remaining K-feldspar fragments. The process advances until the complete destruction of all plagioclase of the rock (both matrix and perthitic grains).

Perthite development as a deformation mechanism

The strong preferential orientation of the perthitic plagioclase veinlets at low angles with the *S*- and *C*-planes indicates that a kinematic rather than crystallographic control acted during perthite development and subsequent feldspar breakdown. This suggests a mechanism of cationic exchange (rather than exsolution) as the probable process of perthite formation in these mylonites [replacement perthites; cf. Smith and Brown (1988) and Pryer and Robin (1995)]. This is also suggested by the flame and vein morphologies (very common in replacement perthites), where the veinlets normally intersect the

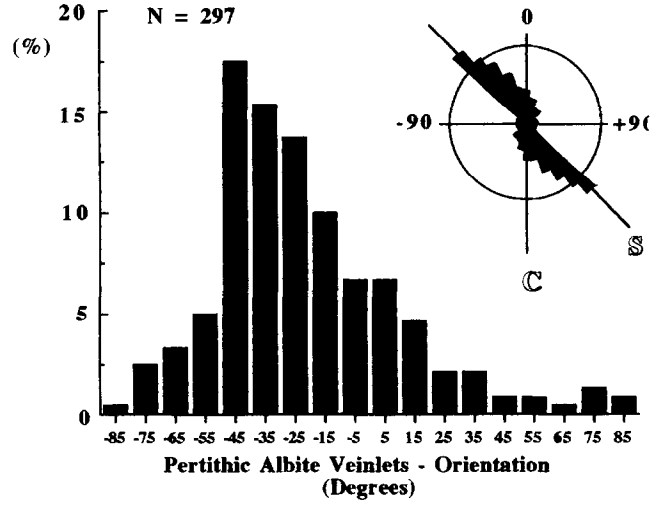

Fig. 7. Histogram showing the orientation of perthitic veinlets in relation to the *S–C* foliations, as seen in sections perpendicular to foliation and parallel to lineation. Note how most of the veinlets have orientations between the *S*- and *C*-foliations. Maximum is at low angle to the *S*-foliation.

grain margins, as expected to occur during external replacement (e.g. Pryer and Robin, 1996). In addition, the very high plagioclase veinlets/K-feldspar volume proportion in the perthitic megacrysts does not favour the exsolution hypothesis. Therefore, the question to be answered is why the replacement front advanced along planes at low angles to the shear plane. The key to answering this question is the volumetric reduction (approximately 7%) that occurs in the unit cell during isostructural replacement of K-feldspar by a plagioclase with composition around An_{10} (see Brown *et al.*, 1984). The replacement along planes sub-parallel to the maximum extension direction implies a volume reduction that will be principally reflected as a contraction in a direction at low angles to the maximum shortening direction of finite strain (Fig. 9). Thus, formation of the veinlets is a deformation mechanism in itself, as the process enables some strain accommodation, principally in the initial stages of deformation when the total volume of perthitic plagioclase can represent up to 60% of the volume of a K-feldspar crystal. If these replacement veinlets were oriented at high angles to the shear plane, it would imply contraction in directions close to the maximum extension of finite strain, which is kinematically improbable in an extensional tectonic framework.

The kinematic framework should also account for the differences between the orientation of the flame perthites investigated in this study, and those studied by Pryer and Robin (1996) which were produced in a compressional tectonic setting. In their model, Pryer and Robin (1996) contend that under differential stresses between 0.3 and 1 GPa, a crystallographically controlled replacement along the Murchison plane (where it is oriented sub-parallel to σ_1) is an efficient way to reduce the strain energy stored elastically in the K-feldspar lattice, as the compressed K-feldspar has lattice dimensions close to those of unstrained albite. In an extensional tectonic setting, however, where σ_1 is vertical and in most cases corresponds to the underburden stress, smaller differential stresses should generally occur (Twiss and Moores, 1992) probably decreasing the importance of elastic strain of K-feldspar in the orientation of the replacement perthites. In this case, the volume reduction associated with the development of replacement perthites may act as an efficient deformation mechanism, leading to a non-crystallographic, preferred orientation of the vein perthites sub-parallel to σ_3, as sketched in Fig. 9. In summary, I suggest that apart from a paleostress indicator, as elegantly modelled by Pryer and Robin (1996), the orientation of the replacement perthites is also controlled by the superimposed tectonic framework, as sketched in Fig. 10.

Another possible control on the orientation of replacement perthites may be exerted by planes of fluid circulation in shear zones that might correspond to *C*-foliations (Hippertt, 1994c), although pervasive fluid migration in other directions may also occur (Bell and Cuff, 1989). The preferential orientation of the replacement perthites at low angles to the S-foliations, however, tells us that the pattern of fluid circulation was not a major control in this perthites, as the S-planes are at high angles to the maximum shortening direction, i.e. in a unfavourable orientation for fluid circulation (Hippertt, 1994c). Replacement controlled by fluid influx along cleavages of K-feldspar would also be another possibility. However, the plagioclase veinlets commonly cross-cut the well-defined cleavage planes, showing that fluid circulation along cleavages apparently did not control the orientation of these replacement perthites.

CHEMICAL CHANGES

Normalized abundances

Chemical changes during deformation were investigated via X-ray fluorescence analysis of major, minor and trace elements in representative samples of the protomylonite and each one of the four microstructural domains within the mylonite zone. Two samples with dimensions at least 20 times the dimensions of the greatest grains of the rock were taken in each domain. An average between the two samples of each domain is given in Table 1. These data are shown in Fig. 11 as profiles of concentration normalized by the composition of the precursor protomylonite.

The most noticeable change is the progressive depletion in Ca and Na towards the centre of the mylonite zone (Fig. 11a). This is corroborated by the progressive disappearance of matrix and perthitic plagioclase with deformation, as discussed above. Phosphorus is also depleted, although not so significantly, with progressive strain. In contrast, K shows a tendency to increase in the

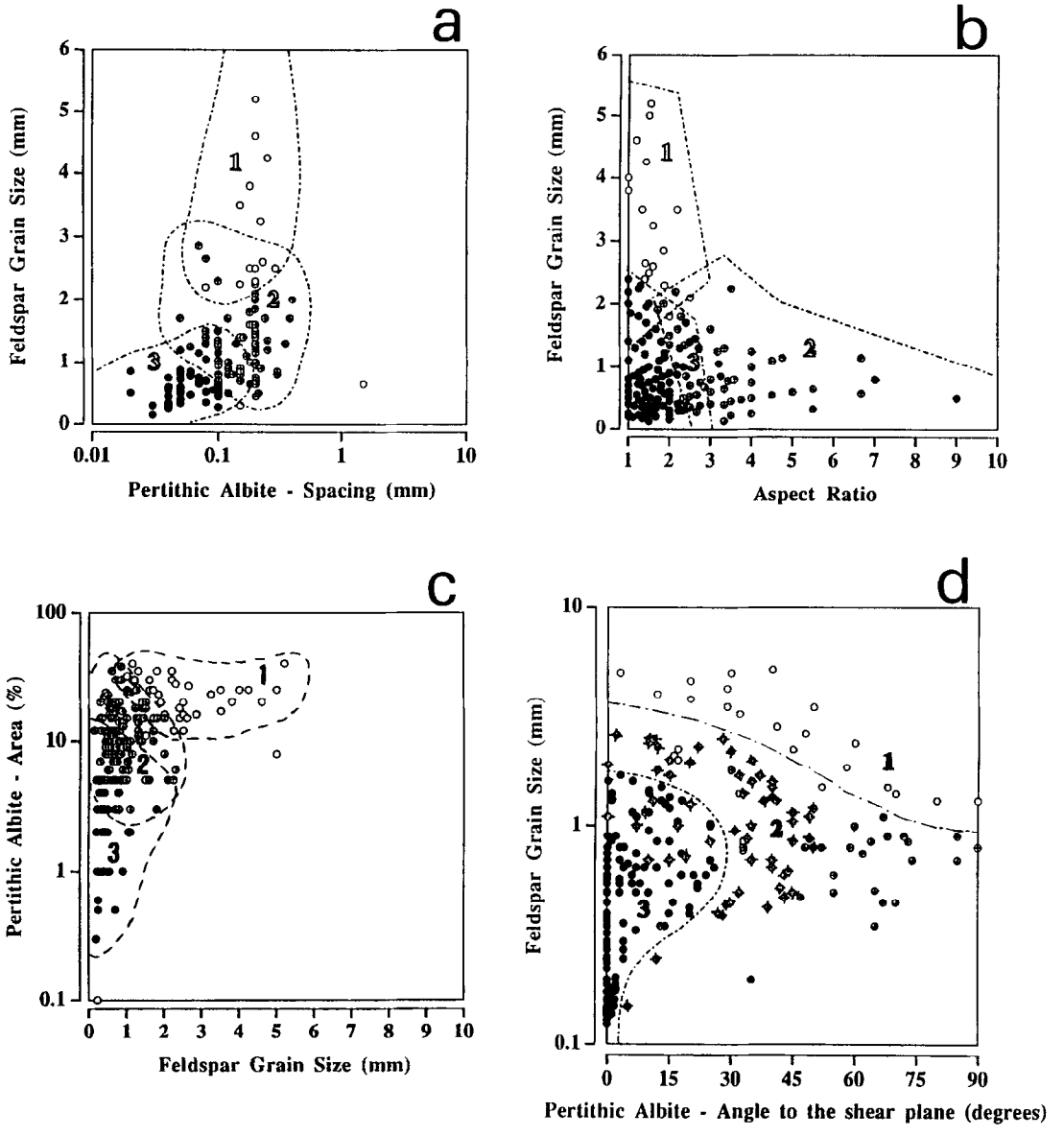

Fig. 8. Characteristics of the perthitic veinlets. In all diagrams, the outlined fields refer to data collected in the protomylonite (1), mylonites from subzones C and D (2) and mylonite from subzone E (3). (a) Variation of the spacing between the perthitic veinlets vs grain size of the host K-feldspar. (b) Variation of aspect ratio of K-feldspar fragments vs grain size. The dramatic increase in the aspect ratio of the fragments in the mylonites of subzones C and D is due to the disruption of the K-feldspar megacrysts along the perthitic veinlets. (c) Variation of the area occupied by the perthitic veinlets in relation to grain size of the host K-feldspar. (d) Variation of the orientation of the veinlets in relation to the K-feldspar grain size. Note that the veinlets become preferentially oriented at low angles to the shear plane with progressive strain. All data collected in sections perpendicular to foliation and parallel to lineation.

mylonite zone. Silicon shows a slight but consistent increase, suggesting that some silicification has taken place in the mylonite zone (Fig. 11b). This is in accordance with the increase in the modal quartz, observed mainly in the central domain. However, Al shows an erratic trend, with a slight (if any) depletion in the mylonite zone.

Figure 11(c & d) shows the variation in the concentration of trace elements that display a tendency toward both increase or decrease with deformation. Only Rb shows a constant positive trend, possibly following the behaviour of K. Strontium follows the geochemical behaviour of Ca and is depleted during plagioclase breakdown. Gallium shows the same slight negative tendency of Al. Cobalt, V and As are also depleted in all domains of the mylonite zone.

Another group of trace elements (Zn, Mn, Sc, Nb and Zr) shows an intriguing profile, characterized by enrichment in the marginal zones and depletion in the centre (a 'zigzag' pattern; Fig. 11e). This behaviour is also followed by the major elements Ti and Mg and, to a lesser extent, by Fe (Fig. 11f), suggesting that lateral migration of components has taken place in this mylonite zone. As most of these components are widely thought to

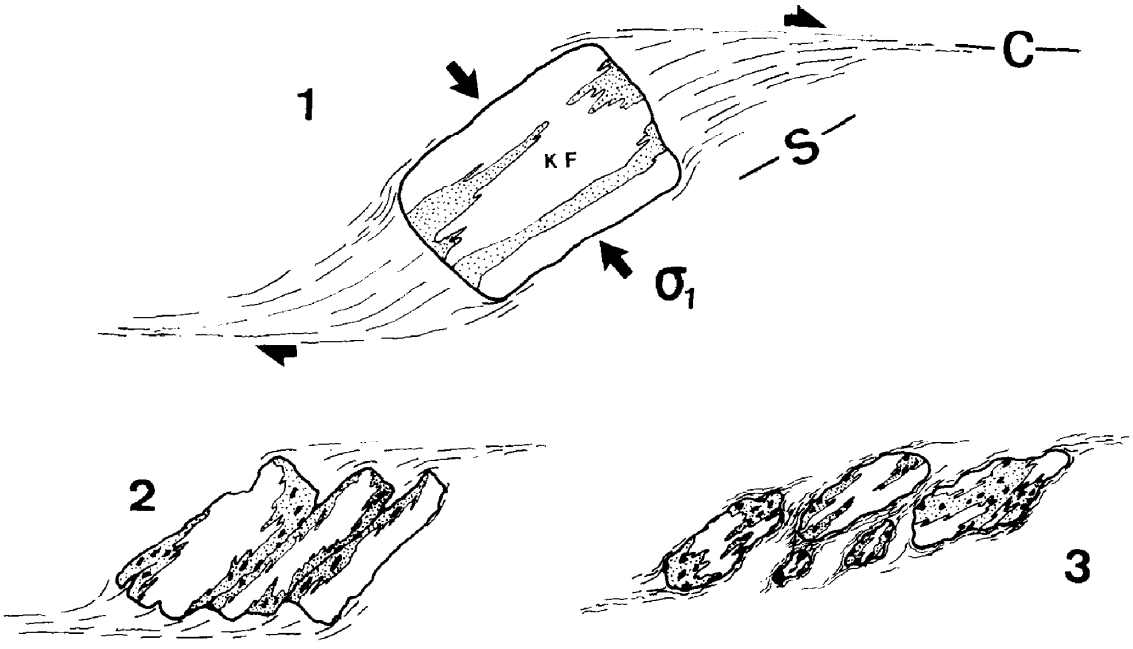

Fig. 9. Sketch illustrating progressive deformation of a K-feldspar megacryst (KF). Stage 1 corresponds to development of replacement perthitic veinlets (stippled) oriented at low angles to the *S*-planes. This kinematically controlled replacement of K-feldspar by the perthitic plagioclase produces an 8% volume reduction parallel to the maximum shortening direction (see text). In stage 2, sericitization (black) of the perthitic plagioclase favors the development of fractures, disrupting the megacryst. Stage 3 illustrates the advanced stage of perthitization and sericitization, where feldspar relics with a rounded outline are immersed in the sericite-rich matrix.

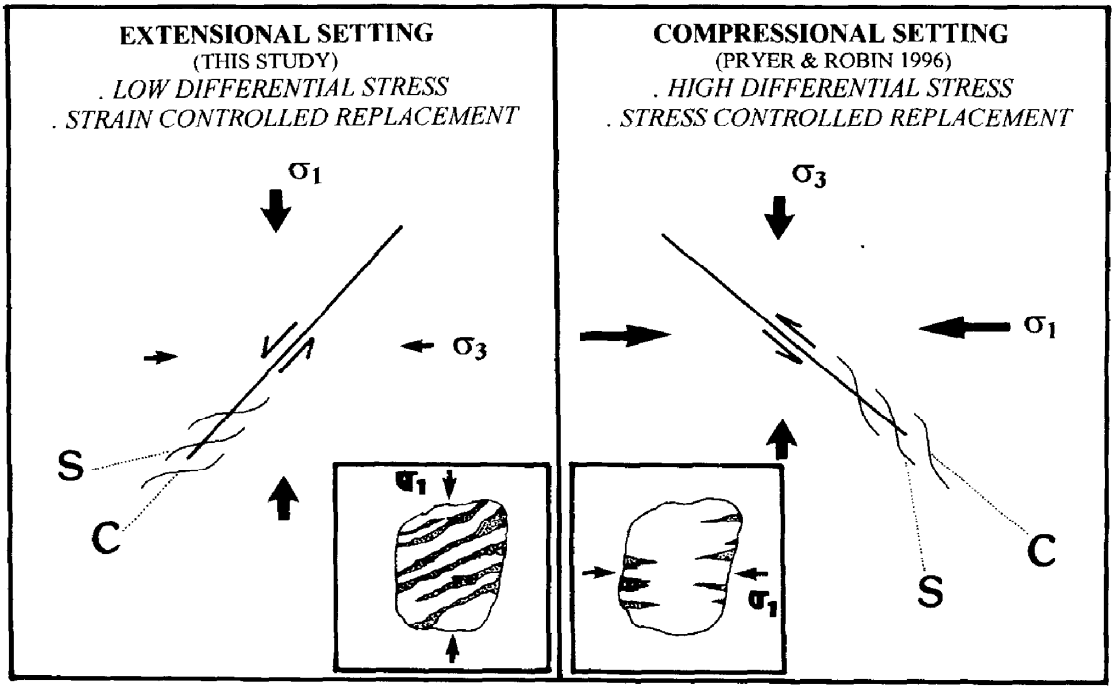

Fig. 10. Sketch showing a comparison between this study and Pryer and Robin (1996) with respect to the state of stress, development of *S*–*C* fabrics and preferred orientation of replacement perthites. The sketches in the corners illustrate typical feldspar grains of the two studies showing replacement perthites of contrasting morphologies and orientations relative to σ_1 (see text).

Table 1. XRF analyses of major and trace elements in the protomylonite (subzone A) and different types of mylonites (subzones B–E) across the 3-m-wide mylonite zone investigated

		Mylonites					
	Protomylonite	Margin East			Centre		Margin West
Subzones	A	B	C	D	E	D	C
SiO_2 (%)	72.02	74.18	74.37	74.80	75.84	79.62	74.98
TiO_2	0.36	0.44	0.34	0.28	0.16	0.25	0.46
Al_2O_3	12.91	13.09	12.63	12.75	13.02	10.45	12.14
Fe_2O_3 tot	1.97	2.39	2.78	2.29	2.29	1.55	2.42
MnO	0.02	0.02	0.03	0.02	0.02	0.02	0.03
MgO	1.36	1.66	1.85	1.17	1.34	1.44	1.97
CaO	0.39	0.20	0.24	0.22	0.05	0.19	0.39
Na_20	1.97	1.08	0.12	0.96	0.06	0.10	0.98
K_2O	5.27	5.44	6.34	5.87	6.01	5.77	5.46
P_2O_5	0.09	0.10	0.08	0.07	0.04	0.06	0.10
LOI	3.23	1.42	1.82	1.48	1.11	1.46	0.91
Ga (ppm)	22	22	21	21	20	14	18
Zn	22	27	28	21	19	21	29
Ni	3	4	5	4	3	4	
Co	24	18	16	16	12	12	17
Mn	171	171	211	144	131	151	213
Cr	4	6	5	7	4	7	12
Sc	6	7	6	5	2	5	8
V	22	23	21	19	12	13	16
As	4	3	3	2	2	2	3
Pb	13	13	7	8	9	12	8
Rb	285	308	367	296	326	279	318
Sr	34	23	14	20	19	20	24
Y	60	36	520	53	32	50	77
Zr	232	339	223	195	125	188	273
Nb	20	25	19	16	18	16	24
Ba	418	433	494	441	407	398	376
Ti	2113	2895	1921	1687	1093	1515	2263
Total (%)	99.77	100.02	100.60	99.91	99.94	100.91	99.84

be insoluble and therefore immobile in hydrothermal events, it is unlikely that they have migrated laterally towards the margins. Instead, migration of major constituents (principally Si, Al and K) from the margins to the centre has probably resulted in the observed profile (see below). This agrees with the low quartz and feldspar content in the margins, and quartz enrichment in the central subzone.

Mass transfer and volume changes during shearing

Inferences on transfer of components in shear zones cannot be made simply by analyzing the relative abundance of the elements in the protolith and deformed rocks, as this gives only a crude idea of the possible chemical changes involved. This is because the system is open to a number of the elements with extremely variable mobilities (i.e. different rates of gain or loss during deformation). Consequently, this commonly leads to volume changes, rendering the actual meaning of the relative abundances obscure. To evaluate which elements have been gained or lost by the system, the first step is to determine which elements have been immobile (usually insoluble elements such as Al, Ti, Zr, P, Y, Nb). This provides a reference frame to determine the degree of gain or loss of the more mobile elements. The determination of the immobile elements can be made graphically by the method of Grant (1986), plotting all the element concentrations (multiplied by scaling factors) in diagrams of concentration of protolith vs rocks with different degrees of metasomatic alteration (Fig. 12). The immobile elements should be on a same straight line passing through the origin in all the diagrams. Such a line, called an isocon, is given by the equation:

$$C^a = (M^p/M^a)C^p, \quad (3)$$

where C is concentration, M is mass, and p and a are superscripts that refer to the protolith and altered rocks, respectively. In Fig. 12, we observe that only Ti and Zr plot on a same isocon in all the diagrams. The small deviations are probably due to analytical errors and/or small heterogeneities in the protolith.

After identifying the immobile elements, the behaviour of each individual element can be evaluated through the variation of its abundance in relation to the immobile element reference frame (Ti in this case; Figs 13 & 14). In this type of graph, the constant mass isocon is a straight line that links the origin to the protolith composition. Elements plotting systematically above and below the constant mass isocon have been gained or lost by the system, respectively. Elements with erratic trends (below the isocon in some diagrams, above in others) have

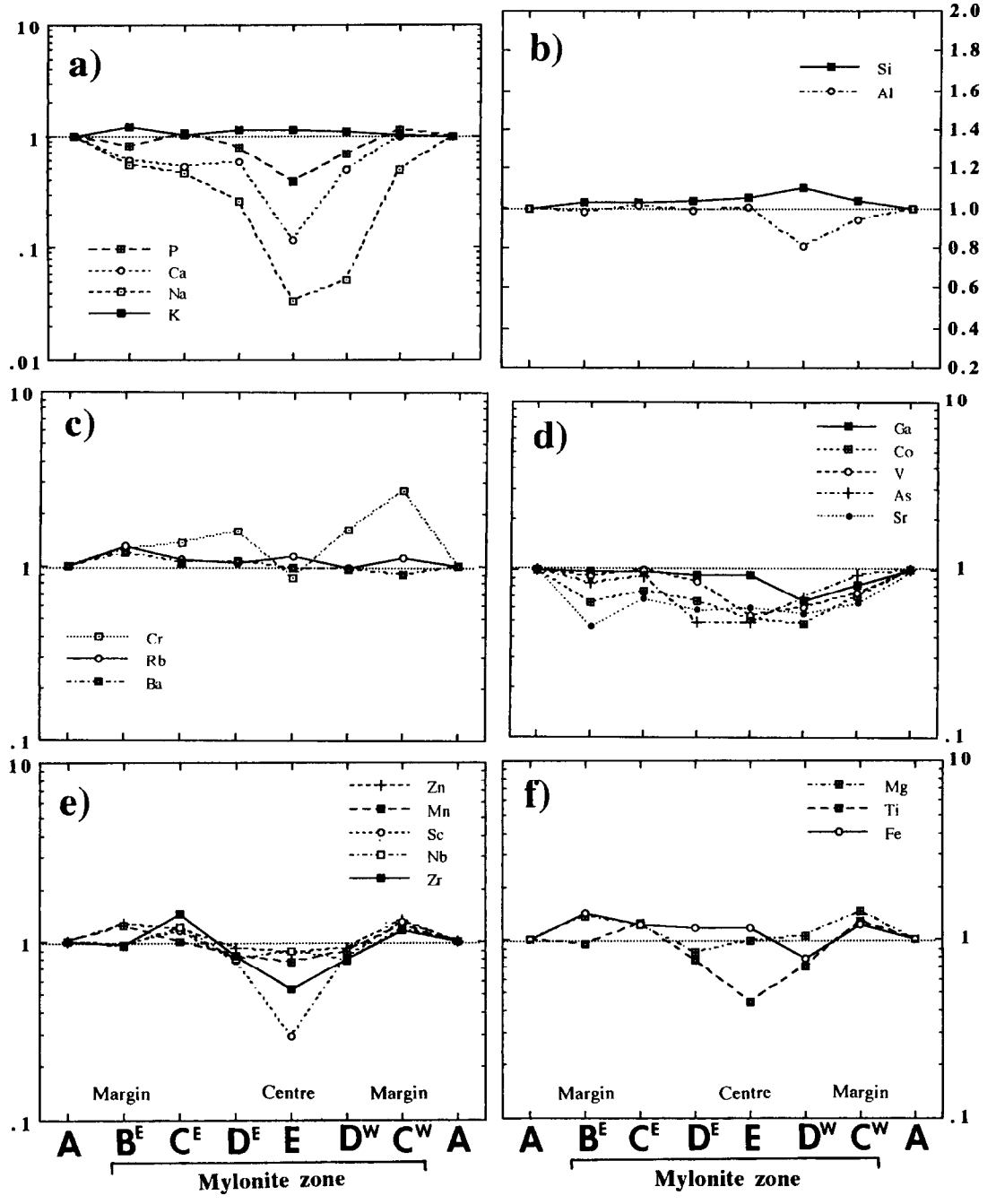

Fig. 11. Diagrams showing concentration of major and trace elements across the mylonite zone normalized by the concentration of the protomylonite. In all diagrams, the vertical axis is 'concentration (mylonite)/concentration (protomylonite)'. The horizontal axis represents a profile across the mylonite zone. Subzone A is the protomylonite. Subzones B to E are the different types of mylonites. Crystal-plastic deformation and reaction-softening increase from A to E. Superscripts E and W refer to the east and west sides of the mylonite zone. (a) Variation of P and alkalis. (b) Variation of Si and Al. (c) Trace elements enriched in the mylonite zone. (d) Trace elements depleted in the mylonite zone. (e) Trace elements showing a 'zigzag' pattern with enrichment in the margins, and depletion in the centre of the mylonite zone. (f) Major elements with a 'zigzag' pattern.

probably migrated laterally within the system, rather than been added to or removed from it. The trajectory of the immobile elements (or those with very low mobility) along the constant mass isocon during the different stages of alteration allows identification of cases of residual enrichment (mass loss) and residual dilution of the immobile elements (mass gain). See Ague (1994) for an extensive discussion on this topic.

The graphs of variation with Ti show that the elements had very different geochemical mobilities and may be split into four distinct groups with respect to their behaviour during shearing. Titanium and Zr were essentially immobile during deformation, as also documented in other low-grade shear zones (O'Hara, 1988; Selverstone *et al.*, 1991; Goddard and Evans, 1995). Phosphorus, Y, Sc and Nb define trends close to the mass

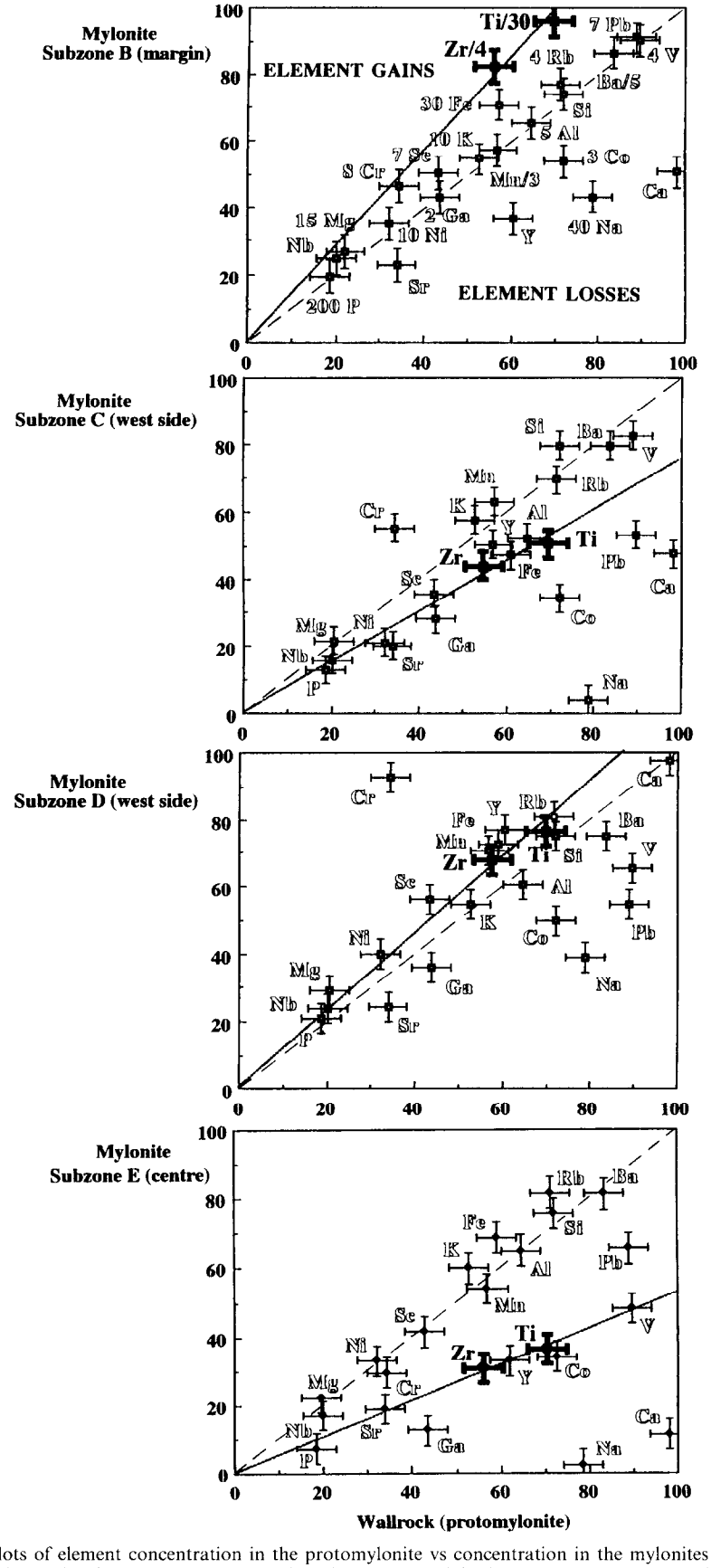

Fig. 12. Plots of element concentration in the protomylonite vs concentration in the mylonites of the different subzones (multiplied by scaling factors). Only Zr and Ti are in a same straight line passing through the origin in all diagrams. These elements define the immobile element reference frame (solid line). The constant mass reference frame (dashed line) is also indicated. Error bars represent one standard deviation.

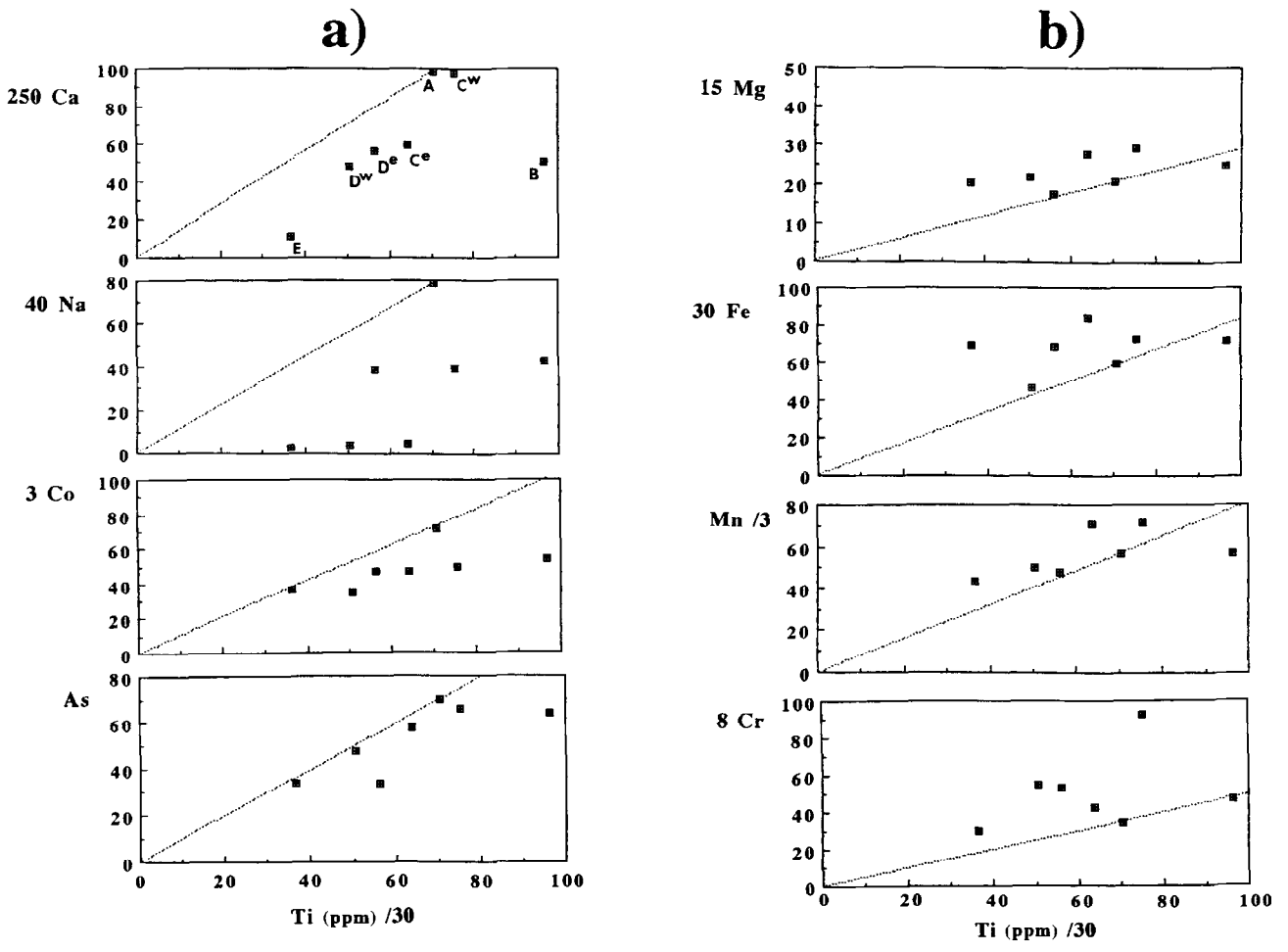

Fig. 13. Diagrams of variation with respect to Ti (immobile element reference frame). Constant mass isocons are indicated in all diagrams (dotted lines). (a) Elements lost in the mylonite zone. (b) Elements added to the mylonite zone.

constant isocon, reflecting a very low mobility, normally restricted to a small scale depletion in highly dissolved marginal subzone B. Aluminium, Si and K display erratic trends, plotting above the isocon in some subzones, but below in others. This also happens with the trace elements Rb and Ga, which possibly follow the geochemical behaviour of K and Al, respectively. Calculations of the mass losses and gains for these elements (T_m; Ague, 1991) separately in the individual subzones can be made using the expression:

$$T_m = (C_i^p/C_i^a)(C_j^a/C_j^p) - 1, \quad (4)$$

where C is concentration, the i and j subscripts refer to immobile and mobile elements, and the p and a superscripts refer to the protolith and altered rocks, respectively. These results, when weighted with the thickness of the subzones, indicated that the amount of Al lost in some subzones corresponds almost exactly to the mass gain in others. This means that deformation in this mylonite zone has been a mass-conservative process for Al, despite its high lateral mobility. However, this is not the case for Si and K. The final balance shows that some amount of Si and K (around 20%) has been introduced in the overall mylonite zone in parallel with an intense lateral mobility between the subzones. This is consistent with the first inferences based in the normalized abundances described above. The interesting fact, however, is that the elements that have migrated laterally are not necessarily those showing a 'zigzag' pattern in the normalized abundance plots (Zn, Mn, Sc, Nb, Zr, Ti). This indicates that lateral migration of the major elements Si, Al and K has created [by domainal residual enrichment and residual dilution; see Ague (1994)] the 'zigzag' pattern shown by other minor and immobile elements.

In order to calculate the global mass change (T_t) in the mylonite zone investigated, I have used the expression

$$T_t = (Cp/Ca) - 1, \quad (5)$$

where Cp and Ca are the concentration of the immobile element used as reference in the protolith and altered rock, respectively (Ague, 1991). Calculations for each one of the deformation subzones gave values varying between -25% in the margin (subzone B) to $+95\%$ in the central subzone E, according to the following mass balance equations:

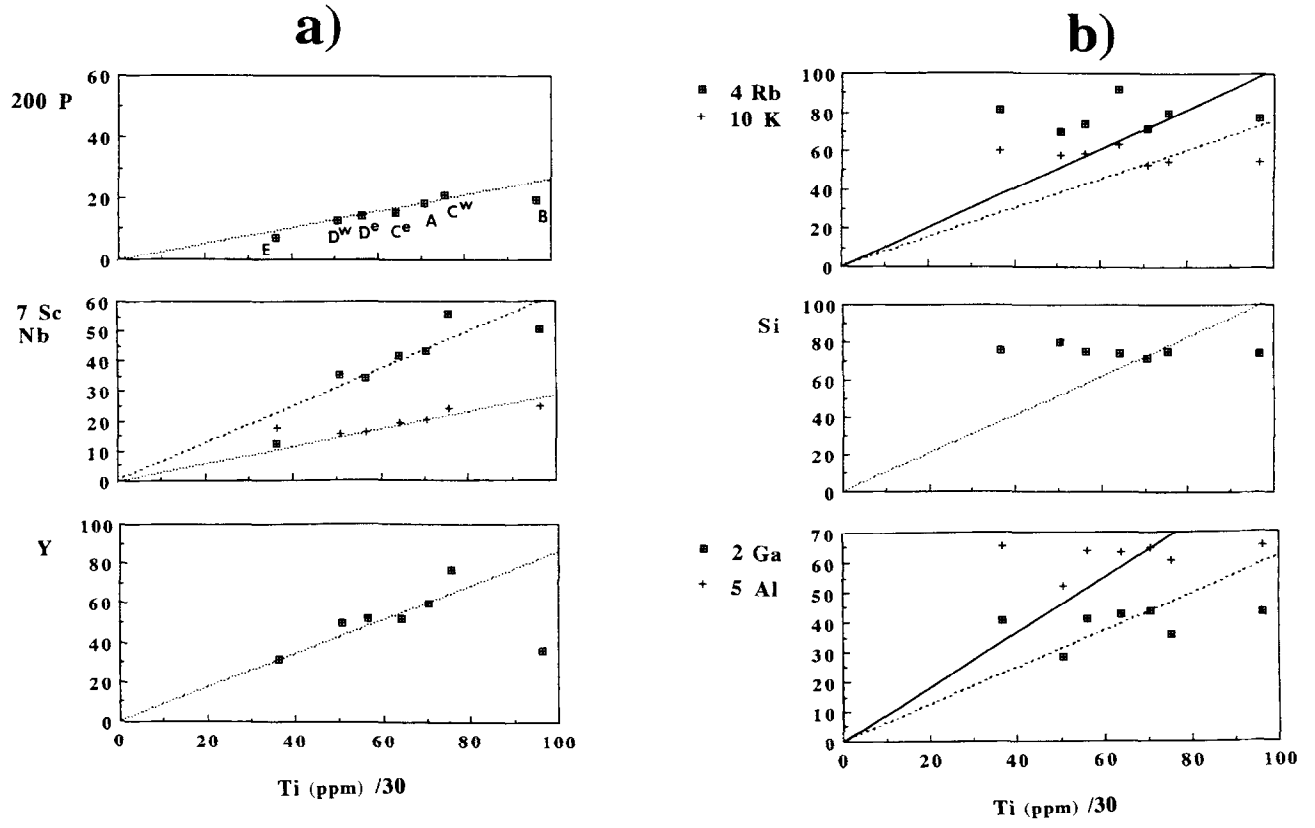

Fig. 14. Diagrams of variation with respect to Ti. (a) Elements with very low mobility. (b) Elements with an erratic trend (lateral migration within the shear zone; see text).

100 g protomylonite − 18.00 g SiO_2 − 3.36 g Al_2O_3
−0.22 g Fe_2O_3−0.15 g MgO−1.18 g Na_2O − 0.24 g CaO
−1.32 g K_2O − 0.02 g P_2O_5−0.02 g MnO
= 75.49 g marginal mylonite subzone B

and

100 g protomylonite + 74.9 g SiO_2 + 12.26 g Al_2O_3
+6.36 g K_2O + 2.48 g Fe_2O_3 + 1.23 g MgO
+0.02 g MnO − 1.85 g Na_2O − 0.30 g CaO
−0.02 g P_2O_5 = 195.08 g central mylonite (subzone E).

These results, when counterweighted by the thickness of the individual subzones, indicate a global mass gain of around 15% in the mylonite zone, which is principally due to the influx of silica, H_2O and K into the system.

The volume changes in the individual subzones (ε) were determined using the simplified expression of Brimhall and Dietrich (1987):

$$\varepsilon = (C^p/C^a)(\rho^p/\rho^a) - 1, \quad (6)$$

where C is the concentration of the immobile element used as reference, ρ is density, and the superscripts p and a refer to protolith and altered rocks, respectively. The density of the rocks was estimated using the modal composition and varies between a minimum of 2.61 in the protomylonite, 2.76 in the central subzone E, to a maximum of 2.95 in the marginal subzone B. These calculations indicated a variation between volume loses of about 35% in the marginal subzone B to a volume gain around 85% in the central subzone E. The global volume change, considering the thickness of the individual domains, indicates a volume gain around 8% in the 3-m-wide mylonite zone investigated. The difference of 7% between mass gain and volume gain can be explained by the higher densities of the tectonites in relation to the protolith, which is principally due to the mica enrichment and influx of high atomic weight elements such as Fe and Mn along with loss of light alkalis.

DISCUSSION

Fluid flow

Fluid circulation in shear zones is a widely recognized phenomenon that accounts for hydration of relatively dry protoliths (e.g. Beach, 1980), and commonly deposits elements of economic interest (Au, for example). The geometry of the fluid movement in shear zones, however, is a controversial subject that is not totally understood, with grain boundaries, fractures and foliations being the most commonly invoked conduits for fluid migration. Most shear zones show evidence that fluid flow is heterogeneous on all scales, where fluid is partitioned

between spaced flow planes that are usually sub-parallel to the shearing plane (Etheridge *et al.*, 1983, 1984). However, local fluid flow along oblique folia (*S*-surfaces, for example) may also occur (Hippertt, 1994c). In general, mica-rich folia in low metamorphic grade tectonites represent in many cases 'solution surfaces' (O'Hara, 1988) where dissolution of more soluble minerals (such as quartz and carbonates) has concentrated residual mica and opaque minerals.

Shear zone margins may represent precursor fractures (Goodwin and Wenk, 1995) and are generally characterized by a strong contrast in porosity and permeability, making these interfaces important routes for fluid flow. This situation is reflected in the noticeable quartz depletion and associated mica enrichment observed in the margins of the studied shear zone, and also in some other shear zone margins (e.g. Selverstone *et al.*, 1991). At higher finite strains, however, when a pervasive set of C-foliations is present, fluid flow is probably partitioned along the parallel mica-rich folia (Hippertt, 1994c).

In the MBSZ, fluid flow was extremely heterogeneous, with the spaced mylonite and phyllonite zones of the MBSZ representing the main routes for syndeformational fluid channelling. However, the pattern of fluid movement in the non-foliated protomylonite domains that separate the distinct mylonite and phyllonite zones is more difficult to visualize, although some fluid activity in these domains is suggested by chloritization of biotite and breakdown of feldspar.

Fluid circulation should also account for lateral mass transfer inside the mylonite zone. The most likely pathways for lateral mass transfer are the extensional gaps oblique to the shear plane. These extensional gaps are easily observed at the microscale in the low strain subzones. They are infilled with quartzose aggregates (sometimes associated with muscovite) showing strong preferred orientation of *c*-axes parallel to the stretching lineation, indicative of an origin by direct precipitation from a solution (Hippertt, 1993).

Volume changes and extensional tectonics

The role of volume loss during deformation/metamorphism has been widely recognized in the last decade as an efficient way to accommodate strain (e.g. Ramsay and Wood, 1973; Wright and Platt, 1982). Volume loss can be produced by different deformation mechanisms, most commonly involving dissolution and solution transfer during foliation formation (e.g. Beutner and Charles, 1984). Reaction-assisted mechanisms, such as retrograde, mica-producing softening reactions may also lead to volume loss via a decrease in the molar volume of the reaction products. Volume loss is recognized as a typical phenomenon of deformation in the upper crust, but may also be important at moderate to high metamorphic conditions (Bell and Cuff, 1989).

A crucial point in this respect is the tectonic context of the deformation zone where volume loss is produced. Previous work on documented cases of volume loss has usually been carried out in schists, mylonites and phyllonites related to compressional tectonics, normally involving thrusting. This seems very reasonable, as in principle, a compressional tectonic framework demands a crustal shortening that may be achieved via volume loss. Under these conditions, pressure solution (Durney, 1972; Rutter, 1983) is possibly favoured due to increasing stress and fluid overpressure at grain contacts [see Shimizu (1995) for discussion]. If the fluid phase is not saturated with respect to local mineral species, dissolved substances can move in solution out of the deformation zone, leading to volume loss.

A totally different scenario should be expected in an extensional tectonic regime. Extensional tectonics may actually be associated with crustal additions (volume gain) as indicated, for example, by the emplacement of granitic plutons in extended crustal blocks. Also, because of the lower mean and differential stresses expected to occur in an extensional setting, porosity development and consequent fluid flow throughout the rock may be facilitated, allowing not only removal, but additions of matter to the shear zone, even considering that most of extensional enviroments in the crust are not necessarily tensile (i.e. σ_1 and σ_3 are generally both positive). Therefore, there is no clear reason for phyllonite and mylonite zones associated with crustal extension to experience significant volume loss. The mass balance calculations made by Jordt-Evangelista *et al.* (1993) indicate only minor volume losses (5–6%) in the phyllonites of the MBSZ, which contrast with the volume losses of up to 80% in documented occurrences of low-metamorphic grade phyllonites formed during thrusting (O'Hara, 1988; O'Hara and Blackburn, 1989).

The protomylonites show microstructures indicative of a very low strain and only small differences in composition relative to the undeformed granitoid that occurs outside the MBSZ (Table 1). Calculations indicate that these protomylonite domains experienced only a minor volume loss (less than 1%) in relation to the undeformed granitoid. This contrasts with the results of O'Hara (1988) who showed that most of the volume loss in the shear zone investigated by him was accommodated in the protomylonites. If we assume an average volume gain around 8% in the mylonites, a volume loss of 6% in the phyllonites and 1% in the protomylonites, and if we consider that the phyllonite/mylonite/protomylonite volume ratio in the MBSZ is around 2:3:9, we can conclude that the overall shear zone experienced a small volume gain (less than 5%), or a nearly isovolumetric shearing. It is suggested that there may be a mechanism of lateral volume compensation between the phyllonite zones (volume loss) and the mylonite zones (volume gain), where the SiO_2 removed from the phyllonites is introduced into the mylonite zones. With regard to this, a major question concerns the influence of the passing fluid in producing the noticeable differences between the evolving microstructure of the phyllonite and mylonite

zones. The differences between volume losses and gains may be even more extreme within the individual mylonite zones. I have found volume changes varying from −35% to +95%, reflecting an intense lateral mass transfer on a metre scale.

One point that needs to be clarified concerns the volume loss involved with perthite formation, which apparently contradicts the overall volume gain experienced by this mylonite zone. However, it should be emphasized that perthite formation is restricted to the protomylonite and marginal subzones, which were subjected to local volume losses. Perthite is in fact absent from the central subzone, where most of volume gain was accommodated.

CONCLUSIONS

By examining domainal deformation mechanisms and chemical transformations in a mylonite zone, this paper emphasizes the role of lateral mass transfer and heterogeneous volume changes during deformation at low metamorphic grade in an extensional tectonic context. The principal conclusions of this study are summarized below.

(1) Formation of replacement perthites occurred in association with plagioclase breakdown, and worked as a deformation mechanism leading to volume loss in the low strain stages of the evolving microstructure. The process was kinematically controlled inducing the perthitic plagioclase veinlets to be oriented at low angles to the shear plane. Subsequent sericitization of the perthitic plagioclase has disrupted host K-feldspar megacrysts.

(2) Lateral mass transfer of major elements (principally Si, Al and K) accounted for the heterogeneous volume changes at outcrop scale. Quartz dissolution and volume loss in the margins, associated with mass gain (silicification) in the centre, are the principal mechanisms of lateral compensation of mass and volume. It is suggested that fluid-assisted mass transfer through extensional gaps accounts for the lateral migration towards the centre of the mylonite zone. Lateral mass transfer also explains the 'zigzag' pattern shown by the immobile elements. The mylonite zone was an open system with respect principally to Na, Ca (moved out) and Fe, Mg and Mn (moved in). The final balance indicates a global mass gain of approximately 15% and a volume gain around 8%.

(3) Shear zones related to extensional tectonics appear to be complex systems in connection with volume changes and mass transfer, as there is no necessity for volume loss to induce a predominant unidirectional process of mass migration out of the shear zone, as normally happens during compressional tectonics. This study has shown that very heterogeneous volume changes with a final balance positive (volume gain), may accompany deformation in extensional shear zones.

Acknowledgements—Financial support for this research was provided by the Brazilian Research Council (CNPq, process 523688/96-2). XRF analyses and SEM observations were carried out in the Earth Sciences Department at James Cook University (Australia) and in the Geology Department at University of Ouro Preto (Brazil). Initial reviews were made by T. Bell, B. Davis, E. Tohver, R. Vernon and R. Wintsch. Constructive journal reviews by C. Mawer and an anonymous referee, and an editorial review by L. Burlini have greatly improved the final version.

REFERENCES

Ague, J. (1991) Evidence for major mass transfer and volume strain during regional metamorphism of pelites. *Geology* **19**, 855–858.

Ague, J. (1994) Mass transfer during Barrovian metamorphism of pelites, south-central Connecticut. I: Evidence for changes in composition and volume. *American Journal of Science* **294**, 989–1057.

Beach, A. (1980) Retrogressive metamorphic processes in shear zones with special reference to the Lewisian complex. *Journal of Structural Geology* **2**, 257–263.

Bell, T. H. and Cuff, C. (1989) Dissolution, solution transfer, diffusion versus fluid flow and volume loss during deformation/metamorphism. *Journal of Metamorphic Geology* **7**, 425–447.

Berthè, D., Choukrone, P. and Jegouzo, P. (1979) Orthogneiss, mylonite and non-coaxial deformation of granites: the example of the South Armorican shear zone. *Journal of Structural Geology* **1**, 31–42.

Beutner, E. C. and Charles, E. G. (1984) Large volume loss during cleavage formation in the Hamburg sequence, Pennsylvania. *Geological Society of America Abstracts with Programs* **16**, 445.

Blacic, J. D. (1975) Plastic deformation mechanisms in quartz: the effect of water. *Tectonophysics* **27**, 171–194.

Brimhall, G. H. and Dietrich, W. E. (1987) Constitutive mass balance relations between chemical composition, volume, density, porosity and strain in metasomatic hydrochemical systems. *Geochimica et Cosmochimica Acta* **51**, 567–587.

Brown, W. L., Openshaw, R. E., McMillan, P. F. and Henderson, M. B. (1984) A review of the expansion behaviour of alkali feldspars: coupled variations in cell parameters and possible phase transitions. *American Mineralogist* **69**, 1058–1071.

Bryant, B. (1966) Formation of phyllonites in the Grandfather mountain area, northeast North Carolina. U.S. Geological Survey, Professional Paper, 550-D: 144–150.

Chemale, F., Rosière, C. A. and Endo, I. (1994) The tectonic evolution of the Quadrilátero Ferrífero, Minas Gerais. *Precambrian Research* **65**, 25–54.

Dipple, G. M., Wintsch, R. P. and Andrews, M. S. (1990) Identification of the scales of differential element mobility in a ductile fault zone. *Journal of Metamorphic Geology* **6**, 645–661.

Dixon, J. and Williams, G. (1983) Reaction softening in mylonites from the Arnaboll thrust Sutherland. *Scottish Journal of Geology* **19**, 157–168.

Durney, D. W. (1972) Solution transfer, an important geological deformation mechanism. *Nature* **235**, 315–317.

Etheridge, M. A., Cox, S. F., Wall, V. F. and Vernon, R. H. (1984) High fluid pressure during regional metamorphism and deformation—Implications for mass transport and deformation mechanisms. *Journal of Geophysical Research* **89**, 4344–4358.

Etheridge, M. A., Wall, V. J. and Vernon, R. H. (1983) The role of the fluid phase during regional metamorphism and deformation. *Journal of Metamorphic Geology* **1**, 205–226.

Fitz Gerald, J. D. and Stünitz, H. (1993) Deformation of granitoids at low metamorphic grade I: Reactions and grain size reduction. *Tectonophysics* **221**, 269–297.

Fry, N. (1979) Random point distributions and strain measurements in rocks. *Tectonophysics* **60**, 89–105.

Fueten, F., Robin, P.-Y. F. and Stephens, R. (1991) A model for the development of a domainal quartz c-axis fabric in a coarse-grained gneiss. *Journal of Structural Geology* **13**, 1111–1124.

Glazner, A. and Bartley, J. (1991) Volume loss, fluid flow and state of strain in extensional mylonites from the central Mojave Desert California. *Journal of Structural Geology* **13**, 587–594.

Goddard, J. and Evans, J. (1995) Chemical changes and fluid–rock interaction in faults of crystalline thrust sheets, northweastern Wyoming, U.S.A. *Journal of Structural Geology* **17**, 533–547.

Goodwin, L. B. and Wenk, H.-R. (1995) Development of phyllonite

from granodiorite: Mechanisms of grain-size reduction in the Santa Rosa mylonite zone California. *Journal of Structural Geology* **17**, 689–708.

Grant, J. A. (1986) The isocon diagram—a simple solution to Gresens equation for metasomatic alteration. *Economic Geology* **81**, 1976–1982.

Griggs, D. T. (1974) A model of hydrolytic weakening in quartz. *Journal of Geophysical Research* **79**, 1653–1661.

Hippertt, J. F. M. (1993) 'V'-pull-apart microstructures: a new shear sense indicator. *Journal of Structural Geology* **15**, 1393–1403.

Hippertt, J. F. M. (1994) Direct observation of porosity in quartzite and phyllonite. *Neues Jahrbuch fur Mineralogie Abhandlungen* **166**, 239–259.

Hippertt, J. F. M. (1994) Microstructures and c-axis fabrics indicative of quartz dissolution in sheared quartzites and phyllonites. *Tectonophysics* **229**, 141–163.

Hippertt, J. F. M. (1994) Grain boundary microstructures in micaceous quartzites: significance for fluid movement and deformation processes in low metamorphic grade shear zones. *Journal of Geology* **102**, 331–348.

Hippertt, J. F. M. and Borba, R. P. (1992) Quartz c-axis fabric differences between porphyroclasts and recrystallized grains: Discussion. *Journal of Structural Geology* **14**, 627–630.

Hippertt, J. F. M., Borba, R. P. and Nalini, H. A. (1992) O contato formação Moeda-Complexo Bonfim: Uma zona de cisalhamento normal na borda oeste do Quadrilátero Ferrífero, MG. *Revista da Escola de Minas* **45**, 32–34.

Hippertt, J. F. M. and Egydio-Silva, M. (1996) New polygonal grains formed by dissolution–redeposition in quartz mylonite. *Journal of Structural Geology* **18**, 1345–1352.

Jamtveit, B., Bucher-Nurminen, K. and Austreim, H. (1990) Fluid controlled eclogitization of granulites in deep crustal shear zones, Bergen Arcs, western Norway. *Contributions to Mineralogy and Petrology* **104**, 184–193.

Janecke, S. and Evans, J. (1988) Feldspar-influenced rock rheologies. *Geology* **16**, 1064–1067.

Jordt-Evangelista, H., Carneiro, M. and Lindenberg, S. F. (1993) Variações químicas do Granito Mamona na zona de cisalhamento do contato com o Supergrupo Minas, Quadrilátero Ferrífero, Minas Gerais. *Anais Simpósio de Geologia de Minas Gerais* **7**, 108–111.

Krohe, A. (1990) Local variations in quartz c-axis orientations in non-coaxial regimes and their significance for the mechanisms of *S–C* fabrics. *Journal of Structural Geology* **12**, 995–1004.

Lee, V. W., Mackwell, S. J. and Brantley, S. L. (1991) The effect of fluid chemistry on wetting textures in Novaculite. *Journal of Geophysical Research* **96**, 10023–10037.

Marquer, D. and Burkhard, M. (1992) Fluid circulation, progressive deformation and mass-transfer processes in the upper crust: the example of basement-cover relationships in the External Crystalline Massifs Switzerland. *Journal of Structural Geology* **14**, 1047–1057.

Marshak, S. and Alkmin, F. F. (1989) Proterozoic contraction/extension tectonics of the southern São Francisco region Minas Gerais, Brazil. *Tectonics* **8**, 555–571.

Marshak, S., Alkmin, F. F. and Jordt-Evangelista, H. (1992) Proterozoic crustal extension and the generation of dome-and-keel structure in an Archaean granite–greenstone terrane. *Nature* **357**, 491–493.

Means, W. (1995) Shear zones and rock history. *Tectonophysics* **247**, 157–160.

Murrell, S. A. F. (1985) Aspects of relationships between deformation and prograde metamorphism that causes evolution of water. In *Metamorphic Reactions: Kinetics, Textures and Deformation*, eds A. B. Thompson and D. C. Rubie, pp. 211–241, Springer, New York.

O'Hara, K. (1988) Fluid flow and volume loss during phyllonitization—an origin for phyllonite in an overthrust setting North Carolina, U.S.A. *Tectonophysics* **156**, 21–36.

O'Hara, K. and Blackburn, W. H. (1989) Volume-loss model for trace element enrichments in mylonites. *Geology* **17**, 21–36.

Orville, P. M. (1962) Alkali metasomatism and feldspars. *Norsk Geologisk Tidsskrift* **42**, 283–316.

Paterson, M. S. (1989) The interaction of water with quartz and its influence in dislocation flow—an overview. In *Rheology of Solids and of the Earth*, eds S. Karato and M. Toriumi, pp. 171–194. Oxford University Press, New York.

Pryer, L. L. and Robin, P.-Y. (1995) Retrograde metamorphic reactions in deforming granites and the origin of flame perthite. *Journal of Metamorphic Geology* **13**, 645–658.

Pryer, L. L. and Robin, P.-Y. (1996) Differential stress control on the growth and orientation of flame perthite: a paleostress-direction indicator. *Journal of Structural Geology* **18**, 1151–1166.

Ramsay, J. G. and Wood, D. S. (1973) The geometric affects of volume change during deformation processes. *Tectonophysics* **16**, 263–277.

Reynolds, S. and Lister, G. (1987) Structural aspects of fluid–rock interactions in detachment zones. *Geology* **15**, 362–366.

Rutter, E. H. (1983) Pressure solution in nature, theory and experiment. *Journal of the Geological Society of London* **40**, 725–740.

Schmid, S. M. and Casey, M. (1986) Complete fabric analysis of some commonly observed quartz c-axis patterns. In *Mineral and Rock Deformation: Laboratory Studies*, eds B. E. Hobbs and H. C. Heard. American Geophysics Union Geophysics Monograph, **36**.

Schorscher, H. D. (1978) Kommatiitos na estrutura 'greenstone belt', Quadrilátero Ferrífero Minas Gerais. *Anais do Congresso Brasileiro de Geologia* **30**, 292–293.

Selverstone, J., Morteani, G. and Staude, J.-M. (1991) Fluid channelling during ductile shearing: transformation of granodiorite into aluminous schist in Tauern Window Eastern Alps. *Journal of Metamorphic Geology* **9**, 419–431.

Shimizu, I. (1995) Kinetics of pressure solution creep in quartz: theoretical considerations. *Tectonophysics* **245**, 121–134.

Simpson, C. (1985) Deformation of granitic rocks across the brittle–ductile transition. *Journal of Structural Geology* **7**, 503–511.

Smith, J. V. and Brown, W. L. (1988) *Feldspar Minerals*. Springer, Berlin.

Stünitz, H. and Fitz Gerald, J. D. (1993) Deformation of granitoids at low metamorphic grade II: granular flow in albite-rich mylonites. *Tectonophysics* **221**, 299–324.

Tullis, T. (1989) Development of preferred orientation due to anisotropic dissolution/growth rates during solution/transfer creep. *EOS* **70**, 457.

Tullis, J. and Yund, R. A. (1989) Hydrolytic weakening of quartz aggregates: The effects of water and pressure on recovery. *Geophysical Research Letters* **16**, 1343–1346.

Twiss, R. and Moores, E. (1992) *Structural Geology*. Freeman, New York.

Urai, J. L., Means, W. D. and Lister, G. S. (1986) Dynamic recrystallization of minerals. In *Mineral and Rock Deformation: Laboratory Studies*, eds B. E. Hobbs and H. C. Heard, pp. 61–99. American Geophysics Union Geophysics Monograph **36**.

van der Molen, I. and Paterson, M. S. (1979) Experimental deformation of partially melted granite. *Contributions to Mineralogy and Petrology* **70**, 299–318.

Watson, E. B. and Brenan, J. M. (1987) Fluids in the lithosphere, 1. Experimentally-determined wetting characteristics of CO_2–H_2O fluids and their implications for fluid transport, host-rock physical properties, and fluid inclusion formation. *Earth and Planetary Science Letters* **85**, 497–515.

White, S. H. (1979) Sub-grain and grain size variation across a shear zone. *Contributions to Mineralogy and Petrology* **70**, 193–202.

White, S. H. and Knipe, R. J. (1978) Transformation- and reaction-enhanced ductility in rocks. *Journal of the Geological Society of London* **135**, 513–516.

Winchester, J. A. and Max, M. D. (1984) Element mobility associated with syn-metamorphic shear zones near Scotchport, NW Mayo, Ireland. *Journal of Metamorphic Geology* **2**, 1–11.

Wintsch, R. P. and Dunning, J. (1985) The effect of dislocation density on the aqueous solubility of quartz and some geologic implications: a theoretical approach. *Journal of Geophysical Research* **90**(B5), 3649–3657.

Wright, T. O. and Platt, L. B. (1982) Pressure solution and cleavage in the Martinsburg shale. *American Journal of Science* **282**, 122–135.